Neurology Asia 2026; 31(1) : 203 – 213

Evaluation of 5-phenylindazoles on LRRK2 inhibition using cellular-based assay and molecular docking

[1]Anis Nadhirah, Khairul Anuar *BSc*, [2]Sek Peng, Chin *PhD*, [3]Chin Fei, Chee *PhD*, [1]Felicita Fedelis, Jusof *PhD*, [1]Hans Xing, Ding *BSc*, [4,5]Ai Huey, Tan *MD PhD*, [4,5]Shen-Yang, Lim *MD*, [1]Yet Hoi, Hong *MBBS PhD*, [1] Lei Cheng, Lit *PhD*

[1]Department of Physiology, Faculty of Medicine, Universiti Malaya, Kuala Lumpur, Malaysia; [2]Department of Pharmaceutical Chemistry, Faculty of Pharmacy, Universiti Malaya, Kuala Lumpur, Malaysia; [3]Nanotechnology and Catalysis Research Centre, Universiti Malaya, Kuala Lumpur, Malaysia; [4]The Mah Pooi Soo & Tan Chin Nam Centre for Parkinson's & Related Disorders, Faculty of Medicine, Universiti Malaya, Kuala Lumpur, Malaysia; [5]Division of Neurology, Department of Medicine, Faculty of Medicine, Universiti Malaya, Kuala Lumpur, Malaysia.

Abstract

LRRK2 has been widely recognised as a critical drug target as it is relevant for both familial and idiopathic cases of Parkinson's disease (PD). Increased LRRK2 kinase activity has been observed in PD patients regardless of their genetic status. This study investigated seventeen 5-phenylindazole derivatives as LRRK2 kinase inhibitors by monitoring Rab10 phosphorylation at Thr73 (a direct LRRK2 substrate) and LRRK2 phosphorylation at Ser935 in HEK293 cells expressing either wild-type or G2019S LRRK2. Molecular docking was used to analyse protein-ligand interactions at the atomic level. In wild-type LRRK2 cells, four small molecules (4h, 4i, 4n and 4o) induced a modest, non-significant inhibition of Rab10 Thr73 phosphorylation (ranging from 27% to 35%), but LRRK2 Ser935 phosphorylation remained unaffected. Whereas no significant inhibition of either LRRK2 Ser935 and Rab10 Thr73 phosphorylation was observed in the LRRK2-G2019S cells treated with any of the 5-phenylindazole derivatives. Computational analysis revealed that these compounds preferentially bind to the open-inactive conformation of LRRK2, a characteristic of type II kinase inhibitors. However, due to their compact molecular scaffolds, these small molecules only partially occupied the extended type II binding pocket, limiting the allosteric engagement necessary for potent inhibition.
In *conclusion*, this structure-activity relationship study demonstrates that while type II binding mode selectivity was modestly achieved, scaffold extension is required to increase molecular size and achieve fuller occupancy of the extended type II pocket.

Keywords: 5-phenylindazoles, LRRK2, Rab10, LRRK2 kinase activity, Parkinson's disease

INTRODUCTION

Parkinson's disease (PD) is the fastest-growing neurological disorder worldwide.[1] With the increasing life span of the world's population due to a better quality of life, a large brunt of this disease burden will be faced by developing nations with under-resourced health infrastructures.[2-4]

PD can be caused by genetic and environmental factors.[1,3] Mutations in the *LRRK2* gene, which expresses the leucine-rich repeat kinase 2 (LRRK2) protein are the commonest cause of autosomal dominant PD, with the *LRRK2* G2019S variant being the most common of these and, like other pathogenic LRRK2 mutations, result in an increased LRRK2 kinase activity.[1,5-7] Interestingly, the enhanced LRRK2 kinase activity is also seen in idiopathic PD (iPD) which comprises about 90% of the overall PD cases, where mutations in *LRRK2* are absent.[8]

LRRK2 is a multi-domain protein, and the kinase domain is where the kinase activity of LRRK2 occurs.[9] Kinase proteins are highly conserved throughout species. They can interchangeably be in an active and inactive state via their catalytic aspartate-phenylalanine-glycine (DFG) motif.[10] Uniquely to LRRK2, the

Address correspondence to: Dr. Lei Cheng, Lit, Department of Physiology, Faculty of Medicine, Universiti Malaya, 50603 Kuala Lumpur, Malaysia. Email: lleicheng@um.edu.my; Dr. Sek Peng, Chin, Department of Pharmaceutical Chemistry, Faculty of Pharmacy, Universiti Malaya, 50603, Kuala Lumpur, Malaysia. Email: spchin@um.edu.my

Date of Submission: 30 September 2025; Date of Acceptance: 10 October 2025

https://doi.org/10.54029/2026jev

phenylalanine in the DFG motif is replaced with tyrosine, making it a DYG motif instead.[11] The DYG motif of LRRK2 kinase adopts a "DYG-in" and "DYG-out" states, when active and inactive, respectively, wherein aspartate is flipped in ("closed-active") and out ("open-inactive") of the active site cleft, which determines ATP binding.[12-15]

Monitoring the LRRK2 at Ser1292 would be an ideal way to measure LRRK2 kinase activity.[16] However, utilising endogenous LRRK2 phosphorylation at Ser1292 as a biomarker is known to be challenging due to its low stoichiometry, which leads to poor antibody detection.[16,17] As an alternative, phosphorylation of LRRK2 at Ser935 (pSer935) has become widely used as a biomarker in LRRK2 inhibitors studies, as it is consistently reduced upon treatment.[18-21] More recently, the discovery of Rab GTPases as direct LRRK2 substrates has led to the identification of Rab10 phosphorylation at Thr73 (pThr73) as a reliable readout for assessing LRRK2 kinase activity.[23-25]

Current PD treatments address the symptoms of the disease and are often accompanied with adverse effects.[1] Significant efforts are focused on developing potent pharmacological treatments targeting the LRRK2 pathway.[26] It is scientifically rationale to target the LRRK2 kinase since increased kinase activity has been observed in both genetic and idiopathic forms of PD.[5] Various potent LRRK2 kinase inhibitors have been developed with different potencies, selectivity, oral availability and brain penetration profiles such as MLi-2.[26] Although selective with desired pharmacological properties, MLi-2 was associated with abnormal cytoplasmic vacuolation in nonhuman primate lung or accumulation of hyaline droplets in rat kidney cells *in vivo*.[27,28] Further understanding and improvements on the small molecules have led pharmaceutical companies to advance their LRRK2 kinase inhibitor candidates to enter clinical trials. Still, none have yet been approved for clinical use.

MLi-2 is a small molecule with an indazole structure that is widely used as a research tool.[26,28] In search of novel LRRK2 inhibitors, we synthesised seventeen 5-phenylindazole derivatives using MLi-2 as a structural reference. These small molecules were evaluated for their ability to reduce phosphorylation levels of LRRK2 pSer935 and Rab10 pThr73 in the cell-based assays. Molecular docking was used to understand the interactions between the 5-phenylindazole derivatives and the LRRK2 kinase at the atomic level.

METHODS

Synthesis of 5-phenylindazole derivatives 4a-q

5-phenyl-3-aminoindazole (3), the corresponding carboxylic acid, 1-[bis(dimethylamino) methylene]-1*H*-1,2,3-triazolo[4,5-*b*]pyridinium 3-oxid hexafluorophosphate (HATU), *N*,*N*-diisopropylethylamine (DIPEA) and *N*,*N*-dimethylformamide (DMF) were added to a round-bottom flask. The flask was stoppered and stirred at room temperature; was the reaction progress was monitored by thin-layer chromatography until all the 5-phenyl-3-aminoindazole was consumed (within 24 hours). Upon completion, the mixture was poured into ice water to yield a solid product, which was collected by filtration and washed with diethyl ether. The product was further purified by column chromatography using a gradient of *n*-hexane/ethyl acetate (4:1 v/v to 1:1 v/v) as eluents.

In silico study

Two-dimensional (2D) structures of 5-phenylindazole derivatives (4a–q) were converted to three-dimensional (3D) using VeraChem (VeraChem LLC, Germantown, MD, USA). Non-kinase domains and ligands, including ATP and GDP of the full-length open-inactive wild-type and G2019S LRRK2 structure (PDB ID: 7LHW and 7LI3, respectively) and the closed-active wild-type LRRK2 kinase model structure (PDB ID: 5U6I), were removed using PyMOL (Schrödinger, LLC). Mutagenesis was generated for the closed-active G2019S LRRK2 kinase model structure.

Docking of the 5-phenylindazole derivatives, MLi-2, and Ponatinib were carried out using HADDOCK with default parameters, and their free binding energies were calculated via PRODIGY.[29,30] The binding modes and interactions between the small molecules and the LRRK2 kinase domain were visualised using Discovery Studio Visualizer 2021 (DSV) (Accelrys, San Diego, CA, USA).

Cell culture

Human Embryonic Kidney (HEK293) cells with either LRRK2-G2019S or LRRK2-WT transfected via the Flp-In™T-REx™ system (Thermo Fisher Scientific, Waltham, MA USA) were used, kindly provided by Professor Dario Alessi from the University of Dundee, United Kingdom. The cells were grown in Dulbecco's modified Eagle medium

(Gibco) with 10% heat-inactivated foetal bovine serum (Sigma Aldrich), 2 mM L-glutamine (Sigma Aldrich), 1% penicillin/streptomycin (Gibco), 15 µg/mL Blasticidin S (Gibco) and 100 µg/mL Hygromycin B (Thermo Fisher Scientific).

MLi-2 and the 5-phenylindazole derivatives were dissolved in dimethyl sulfoxide (DMSO, Sigma Aldrich). MLi-2 and the 5-phenylindazole derivatives were diluted to 200 nM and 5,000 nM, respectively, with the cell culture medium. The HEK293 cells were treated with 1 µg/mL doxycycline (Sigma Aldrich) to induce LRRK2-WT and LRRK2-G2019S expression. After 24 hours of doxycycline treatment, cells were treated with 5-phenylindazole derivatives for 90 minutes.

After treatment, cells were lysed in ice-cold lysis buffer. Lysates were centrifuged at 14,000 rpm at 4°C for 15 minutes. The supernatants were collected and quantified using Bradford assay. Samples were prepared to a concentration of 4 µg/µL with 4xLaemmli buffer and lysis buffer, followed by heating at 95°C for 4 minutes and stored at -20°C.

Western Blot

Gel electrophoresis was conducted at 110 Volts followed by wet transfer to the PVDF membrane at 100 Volts for 120 minutes for LRRK2, and 90 minutes for Rab10 on ice. The transferred membranes were blocked with 5% non-fat skim milk in Tris-buffered saline with 0.1% Tween® 20 (TBST). After blocking, membranes were washed with TBST followed by incubation in the respective primary antibodies at 4°C overnight. Following primary antibodies incubation, membranes were washed before incubating with the respective secondary antibodies at room temperature for 1 hour. Membranes were washed again before imaging with ChemiDoc XRS+ imaging system with Image Lab software (BioRad), visualised using enhanced chemiluminescence. Protein bands were quantified using ImageJ.[31]

Statistical analyses

Quantified immunoblotting data were presented as the mean ± standard error of mean. For the statistical analyses, Kruskal-Wallis with *post hoc* Dunn's test and Benjamini-Hochberg false discovery rate correction were performed using IBM SPSS Statistics for Windows, version 29 (IBM Corp., Armonk, N.Y., USA).

RESULTS

Chemistry

Seventeen 5-phenylindazole derivatives were prepared using the general synthetic methods shown in Figure 1. Briefly, the reaction of commercially available 5-bromo-2-fluorobenzonitrile 1 with hydrazine provided the 5-bromo-3-aminoindazole 2 in 90% yield.[32] Suzuki coupling of 2 with phenyl

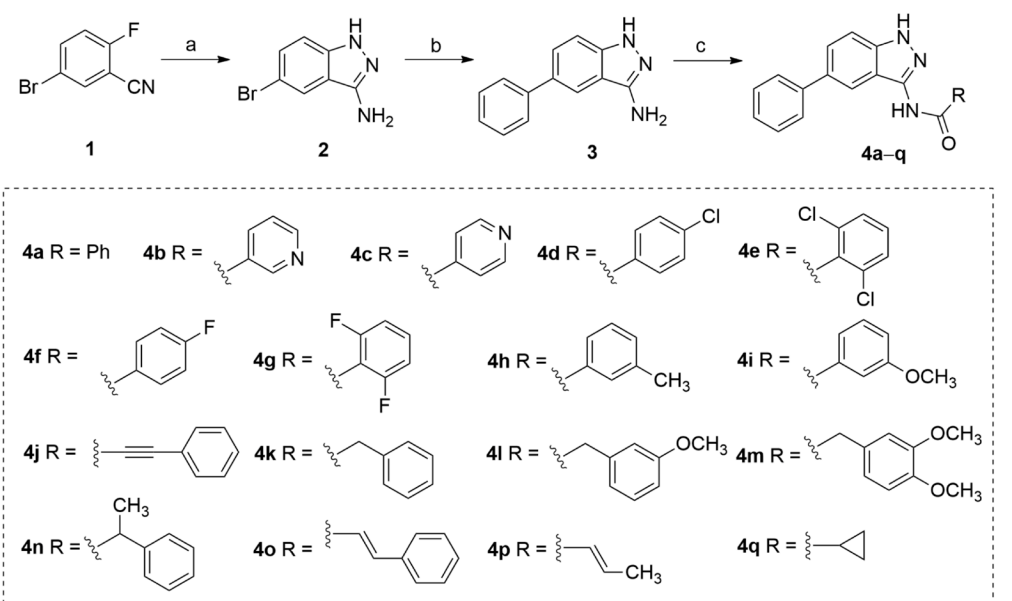

Figure 1. Synthesis of 5-phenylindazoles 4a–q. Reagents and conditions: (a) hydrazine, n-butanol, reflux, 10 h, 90%; (b) phenylboronic acid, Pd(dppf)2Cl2, Cs2CO3, 1,4-dioxane, 100°C, 8 h, 85%; (c) HATU, DIPEA, DMF, rt, 24 h, 55-85%.

boronic acid afforded 5-phenyl-3-aminoindazole 3 in 85% yield. Subsequent HATU-mediated amide coupling between 3 and the corresponding carboxylic acids provided the final products 4a–q in 55-85% yields, all purified by silica gel chromatography. Their structures were confirmed by using nuclear magnetic resonance spectroscopy (^{1}H and ^{13}C) and high-resolution mass spectrometry.[33]

Biology

Effects of 4a–q in the inhibition of LRRK2 pSer935, total LRRK2, Rab10 pThr73 and total Rab10 in LRRK2-G2019S cells

The positive control, MLi-2 significantly inhibits Rab10 Thr73 and LRRK2 Ser935 phosphorylation, confirming the assay validity (Figure 2). None of the small molecules significantly modulates total Rab10 levels (Kruskal-Wallis test, $p > 0.05$; Figure 2a). While 4n reduced total LRRK2 protein levels by approaching 40%, this difference did not reach statistical significance after correcting for multiple comparisons (Benjamini-Hochberg correction, $p > 0.05$; Figure 2b). Furthermore, none of the 5-phenylindazole derivatives inhibited LRRK2 pSer935 and Rab10 pThr73 phosphorylation in the LRRK2-G2019S cells (Kruskal-Wallis test, $p > 0.05$; Figure 2c).

Effects of 4a–q in the inhibition of LRRK2 pSer935, total LRRK2, Rab10 pThr73 and total Rab10 in LRRK2-WT cells

There is no discernible decrease in the levels of total Rab10 protein in the LRRK2-WT cells (Figure 3a), but a marked decrease in total LRRK2 protein levels exceeding 40% was observed with 4e, 4f and 4h (Benjamini-Hochberg correction, $p > 0.05$; Figure 3b). Notably, 4h, 4i, 4n and 4o were observed to inhibit Rab10 pThr73 phosphorylation slightly over 25% and they did not show any inhibition of LRRK2 pSer935 phosphorylation. However, these effects were not statistically significant in LRRK2-WT cells (Kruskal-Wallis, $p > 0.05$; Figure 3c).

In silico

Molecular docking experiments were conducted to predict the optimum protein-ligand binding and their binding free energy ($\Delta G_{prediction}$) to assess the thermodynamic feasibility of the protein-ligand interaction in nature.[33] The more negative the $\Delta G_{prediction}$, the more thermodynamically possible for the protein-ligand interaction to occur. The small molecules 4a–q form stable complexes with the LRRK2 kinase, exhibiting binding free energy like MLi-2, ranging from -7.3 to -8.8 kcal/mol (Supplementary Table 1). Among the seventeen derivatives, fourteen exhibited better $\Delta G_{prediction}$ with both the open-inactive (DYG-out) LRRK2-G2019S and LRRK2-WT kinases than those observed with MLi-2. (Supplementary Table 1).

Despite the lack of significant activity in dephosphorylating Rab10 pThr73, 4h, 4i, 4n, and 4o exhibited favourable $\Delta G_{prediction}$ with the LRRK2 kinase open-inactive conformation. The binding energies of 4h with the open-inactive (DYG-out) and closed-active (DYG-in) conformations of LRRK2 kinase are comparable (-8.2 and -8.3 kcal/mol, respectively, for LRRK2-G2019S, and -7.9 and -8.3 kcal/mol, respectively, for LRRK2-WT; Supplementary Table 1). Despite the minimal differences, 4h forms stable interactions with the open-inactive conformation through various bonds (Figure 4a). 4i demonstrated better binding affinity with the open-inactive conformation (-8.3 kcal/mol for LRRK2-G2019S and -8.1 kcal/mol for LRRK2-WT) compared to MLi-2 while forming an unfavourable bond at Ala81 (corresponding to Ala1950 in the open-inactive LRRK2 kinase structure) in the closed-active (DYG-in) conformation. This unfavourable interaction further supports 4i's selectivity for the open-inactive conformation. Similarly, 4o exhibited stronger binding to the open-inactive conformation (-8.5 kcal/mol for LRRK2-G2019S and -8.1 kcal/mol for LRRK2-WT) relative to MLi-2 (-7.6 and -7.8 kcal/mol, respectively). Also, it formed an unfavourable bond at Ala81 in the closed-active conformation. On the other hand, small molecule 4n displayed superior binding to both the open-inactive (-8.5 and -8.0 kcal/mol for LRRK2-G2019S and LRRK2-WT, respectively) and the closed-active (-8.7 kcal/mol for LRRK2-G2019S) conformations compared to MLi-2, forming stable interactions with both states.

All 4a–q mimics the interactions observed with MLi-2 in the LRRK2 kinase. Ala1950 and Leu2001 (corresponding to Ala81 and Leu132 in the closed-active LRRK2 kinase structure) were found interacting with 4a–q and MLi-2. Based on their favourable binding to the open-inactive LRRK2 kinase conformation, we continued to investigate the interactions of 4h, 4i, 4n and 4o with LRRK2 kinase. Figure 4 shows the 2D and 3D interactions of the four small molecules with the open-inactive (DYG-out) LRRK2-WT kinase. Hydrogen bonds were formed with Arg1957 for 4h, Ser1889, Ala1950, Gly1953 and Arg1957 for

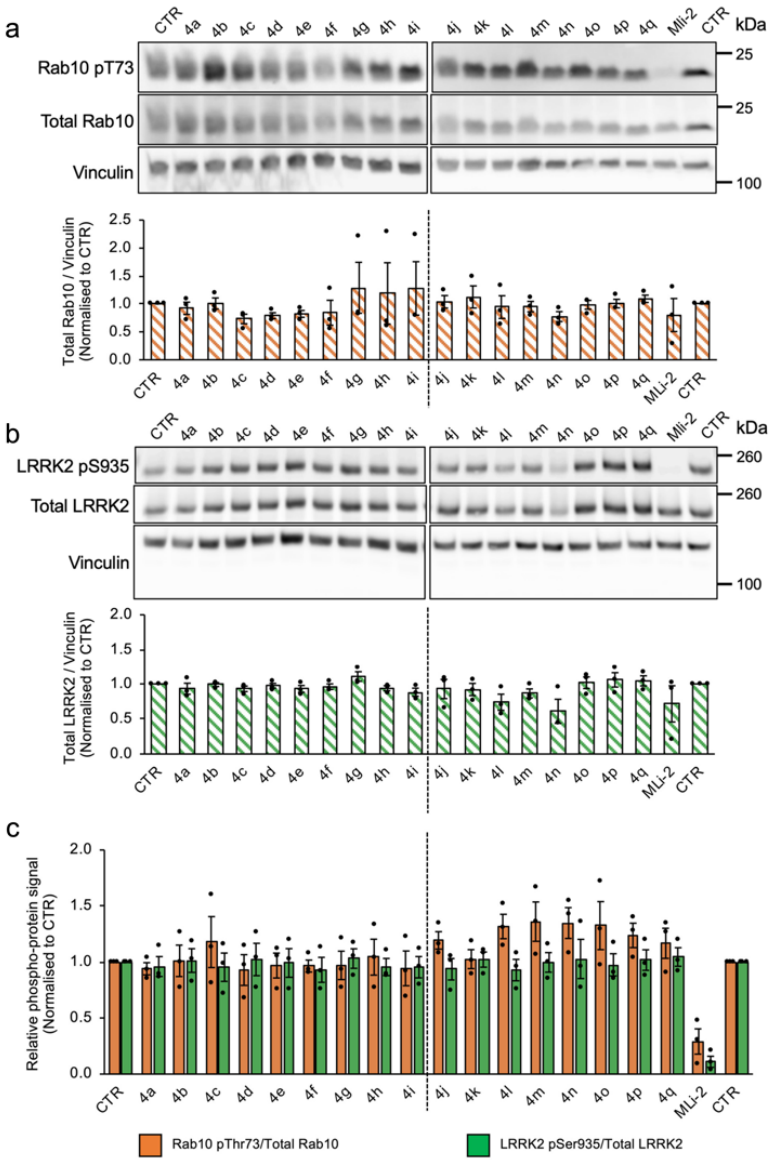

Figure 2. Screening of the seventeen 5-phenylindazole derivatives in LRRK2-G2019S cells. (a) Representative immunoblots of Rab10 pThr73, Total Rab10 and Vinculin, the housekeeping protein of choice. (Bottom panel) Quantified immunoblotting data are presented as ratios of Total Rab10/Vinculin, normalized to respective control (CTR) values. (b) Representative immunoblots of LRRK2 pSer935, Total LRRK2 and Vinculin. (Bottom panel) Quantified immunoblotting data are presented as ratios of Total LRRK2/ Vinculin, normalized to respective CTR values. (c) Relative phospho-protein signal of Rab10 pThr73 and LRRK2 pSer935 ratio to their respective total proteins in LRRK2-G2019S cells. Data presented are normalized to respective CTR values. Data are presented as mean ± standard error of mean from three biological independent experiments, as indicated in the data points. Dashed lines segment the graphs into corresponding blots.

4i, Gly1953 and Ser1954 for 4n, and Asp1887 and Arg1957 for 4o. Aside from the hydrogen bonds, several alkyl, pi-pi, pi-alkyl, pi-cation, pi-sigma and Van der Waals interactions were observed (Figure 4).

Preferential targeting of the open-inactive (DYG-out) conformation by 4h, 4i, 4n, and 4o suggests their potential as type II LRRK2 kinase inhibitors. The superposition of these four small molecules with the type II inhibitor, Ponatinib shows that these small molecules bind only at the LRRK2 kinase active site and not at the extended allosteric site where the type II kinase inhibitor occupies (Figure 5).[34] This is likely because of

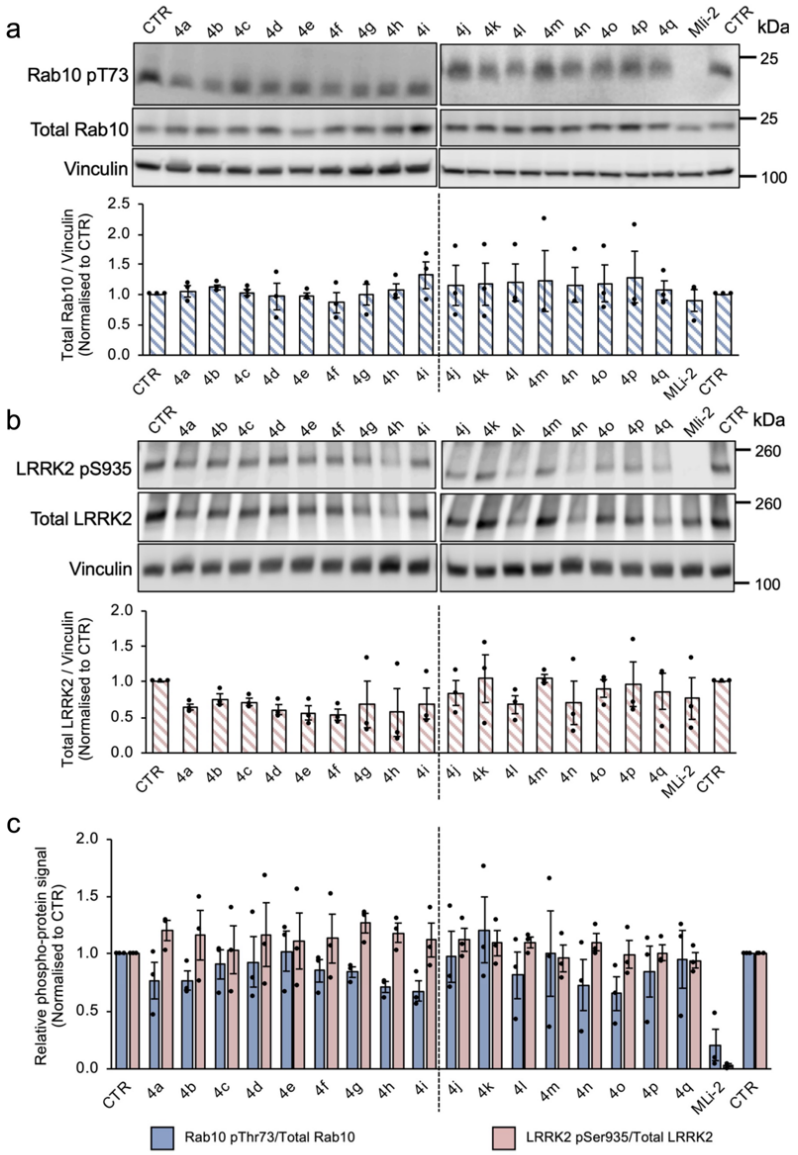

Figure 3. Screening of the seventeen 5-phenylindazole derivatives in LRRK2-WT cells. (a) Representative immunoblots of Rab10 pThr73, Total Rab10 and Vinculin, the housekeeping protein of choice. (Bottom panel) Quantified immunoblotting data are presented as ratios of Total Rab10/Vinculin, normalized to respective control (CTR) values. (b) Representative immunoblots of LRRK2 pSer935, Total LRRK2 and Vinculin. (Bottom panel) Quantified immunoblotting data are presented as ratios of Total LRRK2/Vinculin, normalized to respective CTR values. (c) Relative phospho-protein signal of Rab10 pThr73 and LRRK2 pSer935 ratio to their respective total proteins in LRRK2-WT cells. Data presented are normalized to respective CTR values. Data are presented as mean ± standard error of mean from three biological independent experiments, as indicated in the data points. Dashed lines segment the graphs into corresponding blots.

the smaller size of 4o, 4i, 4h, and 4n (327.38 g/mol, 337.37 g/mol, 341.41 g/mol, and 339.39 g/mol, respectively) compared to other type II kinase inhibitors like Ponatinib (532.60 g/mol).

DISCUSSION

It is challenging for LRRK2 kinase inhibitors to pass clinical trials due to physicochemical limitations and unwanted side effects observed *in vivo*.[26,28,35] Therefore, extensive efforts are

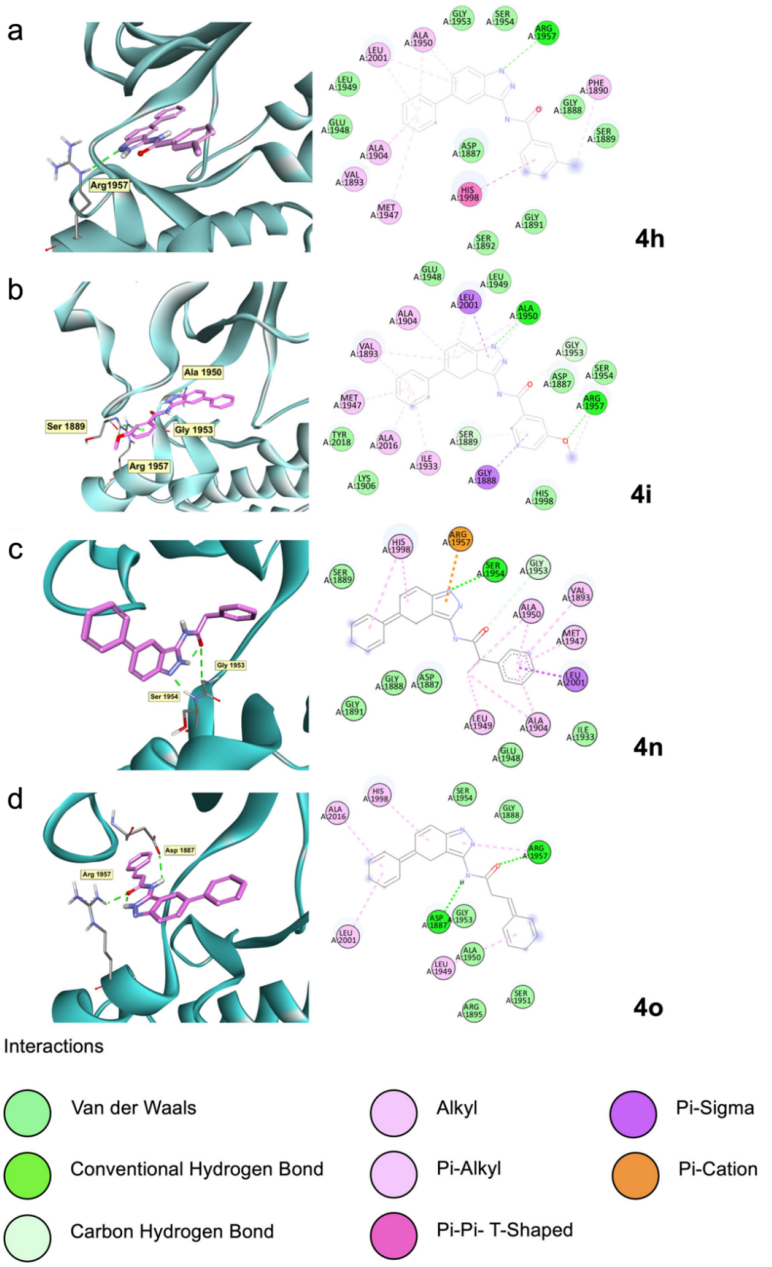

Figure 4. 4h, 4i, 4n and 4o have extensive interaction networks. 3D and 2D interaction diagrams of (a) 4h, (b) 4i, (c) 4n and (d) 4o with the open inactive LRRK2-WT (cyan). The small molecules are shown as pink sticks, amino acids involved in hydrogen bonds are annotated and shown as grey sticks and their bonds are represented as green dotted lines. Oxygen and nitrogen atoms present in the small molecules and amino acids are indicated as red and blue sticks respectively. Parts of the open inactive LRRK2-WT kinase that are blocking the view of the binding site in the 3D interaction diagram are not shown for clarity.

being made in drug discovery for LRRK2 kinase inhibitors.

In this study, seventeen 5-phenylindazole derivatives were synthesised as potential LRRK2 kinase inhibitors. Although these 5-phenylindazole derivatives were synthesised based on the backbone structure of MLi-2 (indazole), none of the small molecules significantly inhibits the LRRK2 phosphorylation in both LRRK2-G2019S and LRRK2-WT cells, as effectively as MLi-2.

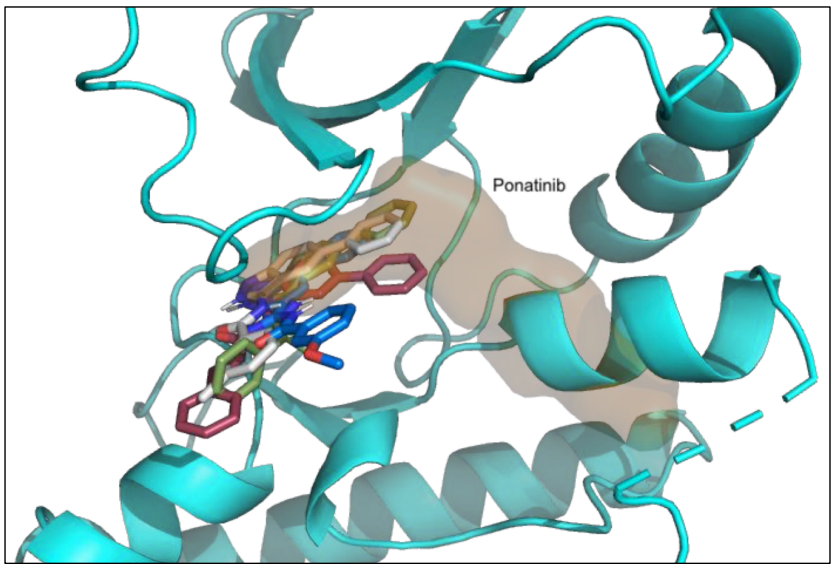

Figure 5. 4h (white sticks), 4i (blue sticks), 4n (green sticks) and 4o (maroon sticks) occupy part of the allosteric site where the type II kinase inhibitor, Ponatinib (orange surface) binds. Oxygen and nitrogen atoms present in the small molecules are indicated as red and dark blue sticks respectively. The open inactive LRRK2 kinase is shown in cyan. Parts of the open inactive LRRK2-WT kinase that are blocking the view of the binding site are not shown for clarity.

Our *in-silico* investigations revealed that the 5-phenylindazole derivatives bind at the same site as the MLi-2 and establish similar interactions with LRRK2 kinase. All the 5-phenylindazole derivatives interact with Ala1950 and Leu2001, which play crucial roles in designing potent LRRK2 kinase inhibitors. Ala1950 is essential for forming hydrogen bonds with inhibitors, while Leu2001 is pivotal for hydrophobic contacts at the ATP binding site.[10,36]

Recent work has established that the distinct binding modes of kinase inhibitors lead to observable differences in their phosphorylation profiles. As reported, type I kinase inhibitors bind to the kinase domain in the closed-active conformation, while type II kinase inhibitors maintain the kinase in the open-inactive conformation.[15] These conformational transitions account for the differential effects on key biomarkers. Type I inhibitors promote the dephosphorylation of LRRK2 Ser935 by stabilizing the active conformation, which consequently reduces 14-3-3 binding. Therefore, they suppress both LRRK2 Ser935 and Rab10 Thr73 phosphorylation. In contrast, type II inhibitors suppress Rab10 Thr73 phosphorylation but do not affect pSer935 levels, as their binding does not induce the 14-3-3 interaction disruption seen with type I inhibitors.[15,37] In our study, 4h, 4i, 4n and 4o induced a non-significant, modest decrease in Rab10 phosphorylation in the wild-type cells, yet LRRK2 Ser935 phosphorylation was unaffected. Interestingly, these small molecules displayed better binding with the open-inactive (DYG-out) LRRK2 kinase. Taken together, these data support the classification of these small molecules as potential type II kinase inhibitor candidates.

While demonstrating potent LRRK2 kinase inhibition, the clinical translation of MLi-2 is hindered by undesirable *in vivo* off-target effects.[28,38] The type I kinase inhibitors are ATP-competitive as they bind to the active site of an active kinase, whereas type II kinase inhibitors bind to a less conserved extended allosteric site, exposed when the kinase is in an inactive state. Hence, type II kinase inhibitors have better selectivity toward the target kinase protein than type I kinase inhibitors.[12,39,40] In the context of LRRK2, type I LRRK2 kinase inhibitors are reported to stabilise the closed-active LRRK2 kinase (DYG-in) and, as a result, enhance LRRK2 binding to microtubules.[11,15] This may cause perturbation to the intracellular trafficking as the binding of LRRK2 acts as a roadblock on the microtubules. In contrast, type II kinase inhibitors stabilise the open-inactive LRRK2 kinase (DYG-out) and prevent the binding of LRRK2 to microtubules.[9,10] Exploring the modification of potential small molecule into type II LRRK2

kinase inhibitor as the next step to improve its potency, may lead to advantageous properties such as reducing off-target effects and rescuing the microtubule-associated intracellular trafficking.

iPD cases comprising approximately 90% of the overall PD cases, reported increased LRRK2 kinase activity without any LRRK2 mutation.[8] Other LRRK2 variants, like G2385R, commonly found among the Asian population, also increased LRRK2 kinase activity despite the mutation positioned at the WD40 domain, outside the kinase domain.[41] Therefore, type II LRRK2 kinase inhibitors can be more beneficial than their type I counterparts, as they can potentially target a larger population of PD patients.

Although statistically insignificant, a marked reduction of total LRRK2 protein was seen in 4n in LRRK2-G2019S cells, as well as 4e, 4f and 4h in LRRK2-WT cells. As LRRK2 has an impact on PD pathogenesis at both the enzymatic (kinase) functions and its scaffolding functions, interests in targeted degradation of LRRK2 as a therapeutic strategy have recently increased. A type of protein degrader – proteolysis-targeting chimera (PROTAC), stimulates the degradation of the protein of interest via the ubiquitin-proteasome system.[42] Liu *et al*. (2022) had discovered and characterised a selective, potent and brain-penetrant LRRK2 PROTAC, whereas Hatcher *et al*. (2023) discovered a degrader molecule based on the structure of MLi-2 that has high potency and selectivity for LRRK2. This may overcome the limitations of type I LRRK2 kinase inhibitors, resulting in better clinical outcomes. Future studies should observe the effect of modified 5-phenylindazoles on the degradation of LRRK2 and the inhibition of phosphorylated LRRK2 and Rab10.

Screening 5-phenylindazole derivatives as potential LRRK2 kinase inhibitors have several limitations. Notably, 4a-q were used at a concentration of 5,000 nM, which is much higher than the 200 nM used for MLi-2. Furthermore, determining the half-maximal inhibitory concentration (IC_{50}) of these derivatives is a crucial step to investigate. However, despite the high concentrations, none of these small molecules effectively inhibited LRRK2 kinase activity, even when compared to a low concentration of MLi-2. Therefore, measuring the IC_{50} after structural optimisation of the 5-phenylindazoles may be a promising approach towards discovering potent type II LRRK2 kinase inhibitors. Based on the known type II kinase inhibitor scaffolds, modifications can be introduced to enhance specificity and binding affinity while transitioning these ligands towards a type II kinase inhibitor profile. Further optimization efforts, informed by the interactions identified here, hold promise for developing more potent and selective LRRK2 inhibitors.

ACKNOWLEDGEMENTS

The authors acknowledge the funding from the Ministry of Higher Education Malaysia under the Fundamental Research Grant Scheme [FRGS/1/2019/SKK08/UM/02/4] and the Universiti Malaya Research Grant [RG392-17ATR]. We would also like to thank Professor Dario Alessi from the Medical Research Council (MRC) Protein Phosphorylation and Ubiquitylation Unit, School of Life Sciences, University of Dundee, United Kingdom for his kindness to provide the HEK293 Flp-InTM T-REx™ LRRK2-G2019S and HEK293 Flp-InTM T-REx™-LRRK2-WT cell lines for this study.

DISCLOSURE

Data availability: The data that support the findings of this study are available from the corresponding authors upon reasonable request.

Financial support: This work was supported by the Ministry of Higher Education Malaysia under the Fundamental Research Grant Scheme [FRGS/1/2019/SKK08/UM/02/4] and the Universiti Malaya Research Grant [RG392-17ATR].

Conflict of interests: None

REFERENCES

1. Bloem BR, Okun MS, Klein C. Parkinson's disease. *Lancet* 2021;397(10291): 2284-303. https://doi.org/10.1016/S0140-6736(21)00218-X
2. Dorsey ER, Bloem BR. The Parkinson Pandemic-A call to action. *JAMA Neurol* 2018; 75(1): 9-10. https://doi.org/10.1001/jamaneurol.2017.3299
3. Lim SY, Tan AH, Ahmad-Annuar A, *et al.* (2019). Parkinson's disease in the Western Pacific Region. *Lancet Neurol* 2019; 18(9): 865-79. https://doi.org/10.1016/S1474-4422(19)30195-4
4. Schiess N, Cataldi R, Okun MS, *et al*. Six action steps to address global disparities in Parkinson disease: A World Health Organization priority. *JAMA Neurol* 2022; 79(9): 929-36. https://doi.org/10.1001/jamaneurol.2022.1783
5. Kalogeropulou AF, Purlyte E, Tonelli F, *et al*. Impact of 100 LRRK2 variants linked to Parkinson's disease on kinase activity and microtubule binding. *Biochem*

J 2022; 479(17): 1759-83. https://doi.org/10.1042/bcj20220161
6. Lesage S, Dürr A, Tazir M, *et al.* LRRK2 G2019S as a cause of Parkinson's disease in North African Arabs. *N Engl J Med* 2006; 354(4): 422-3. https://doi.org/10.1056/NEJMc055540
7. Tolosa E, Vila M, Klein C, Rascol O. LRRK2 in Parkinson disease: challenges of clinical trials. *Nat Rev Neurol* 2020;16(2): 97-107. https://doi.org/10.1038/s41582-019-0301-2
8. Di Maio R, Hoffman EK, Rocha EM, *et al.* LRRK2 activation in idiopathic Parkinson's disease. *Sci Transl Med* 2018; 10(451). https://doi.org/10.1126/scitranslmed.aar5429
9. Deniston CK, Salogiannis J, Mathea S, *et al.* Structure of LRRK2 in Parkinson's disease and model for microtubule interaction. *Nature* 2020; 588(7837): 344-9. https://doi.org/10.1038/s41586-020-2673-2
10. Weng JH, Ma W, Wu J, *et al.* Capturing differences in the regulation of LRRK2 dynamics and conformational states by small molecule kinase inhibitors. *ACS Chem Biol* 2023; 18(4): 810-21. https://doi.org/10.1021/acschembio.2c00868
11. Schmidt SH, Knape MJ, Boassa D, *et al*. The dynamic switch mechanism that leads to activation of LRRK2 is embedded in the DFGψ motif in the kinase domain. *Proc Natl Acad Sci U S A* 2019; 116(30): 14979-88. https://doi.org/10.1073/pnas.1900289116
12. Bukhtiyarova M, Karpusas M, Northrop K, Namboodiri HV, Springman EB. Mutagenesis of p38alpha MAP kinase establishes key roles of Phe169 in function and structural dynamics and reveals a novel DFG-OUT state. *Biochemistry* 2007; 46(19): 5687-96. https://doi.org/10.1021/bi0622221
13. Taylor SS, Kornev AP. Protein kinases: evolution of dynamic regulatory proteins. *Trends Biochem Sci* 2011; 36(2):65-77. https://doi.org/10.1016/j.tibs.2010.09.006
14. Xie T, Saleh T, Rossi P, Kalodimos CG. Conformational states dynamically populated by a kinase determine its function. *Science* 2020; 370(6513). https://doi.org/10.1126/science.abc2754
15. Tasegian A, Singh F, Ganley IG, Reith AD, Alessi DR. Impact of type II LRRK2 inhibitors on signaling and mitophagy. *Biochem J* 2021; 478(19): 3555-73. https://doi.org/10.1042/BCJ20210375
16. Sheng Z, Zhang S, Bustos D, *et al*. Ser1292 autophosphorylation is an indicator of LRRK2 kinase activity and contributes to the cellular effects of PD mutations. *Sci Transl Med* 2012; 4(164): 164ra161. https://doi.org/10.1126/scitranslmed.3004485
17. Rideout HJ, Chartier-Harlin MC, Fell MJ, *et al*. The current state-of-the art of LRRK2-based biomarker assay development in Parkinson's disease. *Front Neurosci* 2020; 14: 865. https://doi.org/10.3389/fnins.2020.00865
18. Fan Y, Howden AJM, Sarhan AR, *et al.* Interrogating Parkinson's disease LRRK2 kinase pathway activity by assessing Rab10 phosphorylation in human neutrophils. *Biochem J* 2018; 475(1): 23-44. https://doi.org/10.1042/BCJ20170803
19. Lis P, Burel S, Steger M, *et al*. Development of phospho-specific Rab protein antibodies to monitor. *Biochem J* 2018; 475(1): 1-22. https://doi.org/10.1042/BCJ20170802
20. Pena N, Richbourg T, Gonzalez-Hunt CP, *et al.* G2019S selective LRRK2 kinase inhibitor abrogates mitochondrial DNA damage. *NPJ Parkinsons Dis* 2024; 10(1): 49. https://doi.org/10.1038/s41531-024-00660-y
21. Perera G, Ranola M, Rowe DB, Halliday GM, Dzamko N. Inhibitor treatment of peripheral mononuclear cells from Parkinson's disease patients further validates LRRK2 dephosphorylation as a pharmacodynamic biomarker. *Sci Rep* 2016; 6: 31391. https://doi.org/10.1038/srep31391
22. Dzamko N, Deak M, Hentati F, *et al.* Inhibition of LRRK2 kinase activity leads to dephosphorylation of Ser(910)/Ser(935), disruption of 14-3-3 binding and altered cytoplasmic localization. *Biochem J* 2010; 430(3): 405-13. https://doi.org/10.1042/BJ20100784
23. Atashrazm F, Hammond D, Perera G, *et al*. LRRK2-mediated Rab10 phosphorylation in immune cells from Parkinson's disease patients. *Mov Disord* 2019; 34(3): 406-15. https://doi.org/10.1002/mds.27601
24. Steger M, Tonelli F, Ito G, *et al*. Phosphoproteomics reveals that Parkinson's disease kinase LRRK2 regulates a subset of Rab GTPases. *Elife* 2016; 5:e12813. https://doi.org/10.7554/eLife.12813
25. Steger M, Diez F, Dhekne HS, *et al.* Systematic proteomic analysis of LRRK2-mediated Rab GTPase phosphorylation establishes a connection to ciliogenesis. *Elife* 2017; 6: e31012. https://doi.org/10.7554/eLife.31012
26. Fell MJ, Mirescu C, Basu K, *et al*. MLi-2, a potent, selective, and centrally active compound for exploring the therapeutic potential and safety of LRRK2 kinase inhibition. *J Pharmacol Exp Ther* 2015; 355(3): 397-409. https://doi.org/10.1124/jpet.115.227587
27. Andersen MA, Wegener KM, Larsen S, *et al.* PFE-360-induced LRRK2 inhibition induces reversible, non-adverse renal changes in rats. *Toxicology* 2018; 395: 15-22. https://doi.org/10.1016/j.tox.2018.01.003
28. Baptista MAS, Merchant K, Barrett T, *et al.* LRRK2 inhibitors induce reversible changes in nonhuman primate lungs without measurable pulmonary deficits. *Sci Transl Med* 2020; 12(540). https://doi.org/10.1126/scitranslmed.aav0820
29. van Zundert GCP, Rodrigues JPGLM, Trellet M, *et al*. The HADDOCK2.2 web server: User-friendly integrative modeling of biomolecular complexes. *J Mol Biol* 2016; 428(4): 720-5. https://doi.org/10.1016/j.jmb.2015.09.014
30. Vangone A, Schaarschmidt J, Koukos P, *et al*. Large-scale prediction of binding affinity in protein-small ligand complexes: the PRODIGY-LIG web server. *Bioinformatics* 2019; 35(9): 1585-7. https://doi.org/10.1093/bioinformatics/bty816
31. Schneider CA, Rasband WS, Eliceiri KW. NIH Image to ImageJ: 25 years of image analysis. *Nat Methods* 2012; 9(7): 671-5. https://doi.org/10.1038/nmeth.2089
32. Tobuse AJ, Law CSW, Thy CK, James JJ, Chee CF, Yeong KY. Indazole derivatives as selective inhibitors of butyrylcholinesterase with effective blood-brain-barrier permeability profile. *Med Chem Res* 2024;

33: 298-307. https://doi.org/10.1007/s00044-023-03179-8
33. Dar HA, Waheed Y, Najmi MH, *et al.* Multiepitope subunit vaccine design against COVID-19 based on the spike protein of SARS-CoV-2: An *in silico* analysis. *J Immunol Res* 2020; 8893483. https://doi.org/10.1155/2020/8893483
34. Zhu H, Hixson P, Ma W, Sun J. Pharmacology of LRRK2 with type I and II kinase inhibitors revealed by cryo-EM. *Cell Discov* 2024; 10(1): 10. https://doi.org/10.1038/s41421-023-00639-8
35. Thakur G, Kumar V, Lee KW, Won C. Structural insights and development of LRRK2 inhibitors for Parkinson's disease in the last decade. *Genes* (Basel) 2022; 13(8). https://doi.org/10.3390/genes13081426
36. Tan S, Zhang Q, Wang J, *et al*. Molecular modeling study on the interaction mechanism between the LRRK2 G2019S mutant and type I inhibitors by integrating molecular dynamics simulation, binding free energy calculations, and pharmacophore modeling. *ACS Chem Neurosci* 2022; 13(5): 599-612. https://doi.org/10.1021/acschemneuro.1c00726
37. Martinez Fiesco JA, Beilina A, Alvarez de la Cruz A, *et al.* 14-3-3 binding maintains the Parkinson's associated kinase LRRK2 in an inactive state. *Nat Commun* 2025; 16(1):7226. https://doi.org/10.1038/s41467-025-62337-1
38. Bryce DK, Ware CM, Woodhouse JD, *et al*. Characterization of the onset, progression, and reversibility of morphological changes in mouse lung after pharmacological inhibition of leucine-rich kinase 2 kinase activity. *J Pharmacol Exp Ther* 2021; 377(1): 11-9. https://doi.org/10.1124/jpet.120.000217
39. Hubbard SR, Wei L, Ellis L, Hendrickson WA. Crystal structure of the tyrosine kinase domain of the human insulin receptor. *Nature* 1994; 372(6508): 746-54. https://doi.org/10.1038/372746a0
40. Liu Z, Bryant N, Kumaran R, *et al*. LRRK2 phosphorylates membrane-bound Rabs and is activated by GTP-bound Rab7L1 to promote recruitment to the trans-Golgi network. *Hum Mol Genet* 2018; 27(2): 385-95. https://doi.org/10.1093/hmg/ddx410
41. Leandrou E, Markidi E, Memou A, Melachroinou K, Greggio E, Rideout HJ. Kinase activity of mutant LRRK2 manifests differently in hetero-dimeric vs. homo-dimeric complexes. *Biochem J* 2019; 476(3): 559-79. https://doi.org/10.1042/bcj20180589
42. Békés M, Langley DR, Crews CM. PROTAC targeted protein degraders: the past is prologue. *Nat Rev Drug Discov* 2022; 21(3): 181-200. https://doi.org/10.1038/s41573-021-00371-6

Supplementary Table 1: Predicted free binding energy ($\Delta G_{prediction}$) of 5-phenylindazole small molecules with LRRK2 kinase

	$\Delta G_{prediction}$ (kcal/mol)			
Small molecule	**Open inactive LRRK2-G2019S**	**Open inactive LRRK2-WT**	**Closed active LRRK2-G2019S**	**Closed active LRRK2-WT**
4a	–8.4	–8.2	–7.9	–8.2
4b	–8.2	–8.1	–7.8	–8.2
4c	–8.3	–8.3	–7.9	–8.0
4d	–8.5	–7.8	–8.3	–8.1
4e	–8.4	–8.3	–8.2	–8.3
4f	–8.2	–8.1	–7.9	–7.9
4g	–8.6	–8.0	–8.1	–8.0
4h	–8.2	–7.9	–8.3	–8.3
4i	–8.3	–8.1	–8.0	–8.0
4j	–8.7	–7.7	–8.0	–8.2
4k	–8.4	–8.2	–8.5	–8.3
4l	–8.5	–8.0	–8.2	–8.2
4m	–8.8	–8.4	–8.3	–8.1
4n	–8.5	–8.0	–8.7	–7.7
4o	–8.5	–8.1	–8.1	–7.8
4p	–7.8	–7.9	–7.6	–8.3
4q	–7.9	–7.3	–7.7	–8.1
MLi-2	–7.6	–7.8	–8.3	–8.2